

## Electrochemical Characteristics and Microstructures of Activated Carbon Powder Supercapacitors for Energy Storage

Tayara Correia Gonsalves<sup>1</sup>, Franks Martins Silva<sup>2</sup>, Ligia Silverio Vieira<sup>2</sup>,  
Julio Cesar Serafim Casini<sup>2,a\*</sup>, Rubens Nunes de Faria<sup>1,b</sup>

<sup>1</sup>Materials Science and Technology Center, Nuclear and Energy Research Institute, University of São Paulo, SP 05508-900, Brazil.

<sup>2</sup>Federal Institute of Education, Science and Technology of Rondônia, Campus Calama, RO 76820-441, Brazil.

<sup>a</sup>julio.casini@ifro.edu.br, <sup>b</sup>rfaria@ipen.br

Av. Calama, 4985, Flodoaldo Pontes Pinto, 76820-441, Porto Velho, Rondonia RO, Brazil

**Keywords:** supercapacitor self-discharge, energy storage, scanning electron microscopy.

**Abstract:** In recent years, extensive investigations have focused on the study and improvement of supercapacitor electrode materials. The electric devices produced with these materials are used to store energy over time periods ranging from seconds to several days. The main factor that determines the energy storage period of a supercapacitor is its self-discharge rate, i.e., the gradual decrease in electric potential that occurs when the supercapacitor terminals are not connected to either a charging circuit or electric load. Self-discharge is attenuated at lower temperatures, resulting in an increased energy storage period. This paper addresses the temperature-dependence of self-discharge via a systematic study of supercapacitors with nominal capacitances of 1.0 and 10.0 F at DC potentials of 5.5 and 2.7 V, respectively. The specific capacitances, internal resistances, and self-discharge characteristics of commercial activated carbon electrode supercapacitors were investigated. Using cyclic voltammetry, the specific capacitances were determined to be 44.4 and 66.7 Fg<sup>-1</sup> for distinct carbon electrode supercapacitors. The self-discharge characteristics were investigated at both room temperature and close to the freezing point. The internal resistances of the supercapacitors were calculated using the discharge curves at room temperature. The microstructures of the electrode materials were determined using scanning electron microscopy.

### Introduction

In recent years, extensive investigations have focused on the study and improvement of supercapacitor electrode materials [1-7]. The electric devices produced with these materials are used to store energy over time periods ranging from seconds to several days [7]. The main factor that determines the energy storage period of a supercapacitor is its self-discharge rate, i.e., the gradual decrease in the electric potential that occurs when the supercapacitor terminals are not connected to either a charging circuit or electric load [7]. The self-discharge characteristics and lifetimes of supercapacitors are dramatically dependent on the temperature: Self-discharge is attenuated at lower temperatures, resulting in an increased lifetime. This paper addresses the temperature-dependence of self-discharge via a systematic study of supercapacitors with nominal capacitances of 1.0 and 10.0 F at DC potentials of 5.5 and 2.7 V, respectively.

### Experimental

Two types of activated carbon electrode supercapacitors were studied in this investigation. The first type was a disc-type 1 F supercapacitor comprising four electrodes in a serial orientation (two cells) that was used to achieve a maximum nominal working potential of 5.5 V, with each electrode containing an active carbon mass of 0.09 g. Because each electrode intrinsically contains an electrical double layer, the nominal specific capacitance of this disc-type supercapacitor was calculated to be 44.4 Fg<sup>-1</sup> (i.e., 4 × 1 F/0.09 g). The second type was a tubular-type 10 F

supercapacitor comprising two electrodes in a serial orientation with a maximum nominal working potential of 2.7 V and masses of 0.3 g each. The nominal specific capacitance of this tubular-type supercapacitor was calculated to be  $66.7 \text{ Fg}^{-1}$  ( $2 \times 10 \text{ F}/0.3 \text{ g}$ ). The electrochemical characteristics of the carbon electrodes were investigated using a digital Arbin analyzer. The specific capacitance was determined from the cyclic voltammetry (CV) curves using equation (1), as follows:

$$C_s = \frac{\int_{V_i}^{V_f} i(V) dV}{2\nu(V_f - V_i)} \quad (1)$$

The specific capacitance was determined using the constant current discharge method based on the discharge curve [8,9] (galvanostatically charged/discharged at  $1 \text{ mAF}^{-1}$ ), as per equation (2).

$$C_s = \frac{I \Delta t}{\Delta V_m} \quad (2)$$

The equivalent series resistance (ESR) was determined by discharging the fully charged carbon electrodes at  $1 \text{ mAF}^{-1}$  and reducing the current to zero. Using equation (3), the ESR was calculated from the initial potential ( $V_i$ ) and the potential after 5 s of null current ( $V_f$ ) [1].

$$\text{ESR} = \frac{V_f - V_i}{I} \quad (3)$$

The internal equivalent parallel resistance (EPR) was determined by charging the supercapacitors to  $V_o$  for 30 min and allowing them to self-discharge to obtain the values required for the following equation [10]:

$$\text{EPR} = \frac{-t}{C \ln \left( \frac{V}{V_o} \right)} \quad (4)$$

Where  $V$  is the final potential after a period of self-discharge ( $t$ ).

The microstructures of the electrode materials were investigated using a scanning electron microscope (Hitachi) along with chemical microanalyses via energy dispersive X-ray analysis. The electrode material was subjected to a high vacuum ( $10^{-6}$  mbar) prior to the microstructure investigations in order to eliminate any remnant electrolyte residue from the microscope chamber.

## Results and Discussion

Figures 1 and 2 show the room-temperature CV curves for the  $1 \text{ F}/5.5 \text{ V}$  and  $10 \text{ F}/2.7 \text{ V}$  supercapacitors at distinct scan rates. The performance of the latter supercapacitor is superior to that of the former: The CV curves of the  $1 \text{ F}$  supercapacitor resemble those of an ideal supercapacitor. This behavior is more striking at higher scan rates and reveals that the ESR and EPR values of the  $1 \text{ F}$  supercapacitor are substantially higher than those of the  $10 \text{ F}$  supercapacitor.

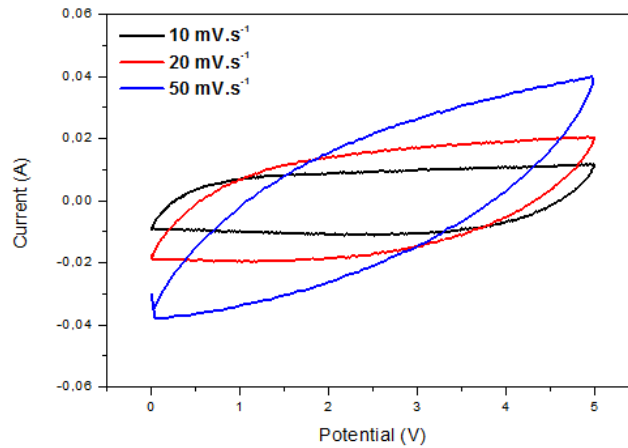


**Fig. 1.** Cyclic voltammetry curves of the 1 F/5.5 V disc-type supercapacitor at distinct scan rates.

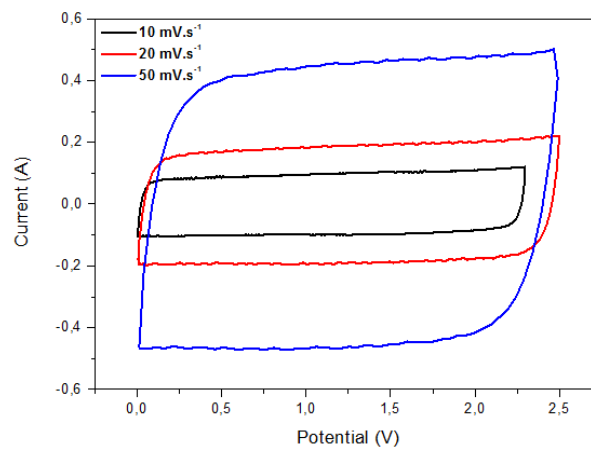


**Fig. 2.** Cyclic voltammetry curves of the 10 F/2.7 V tubular-type supercapacitor at distinct scan rates.

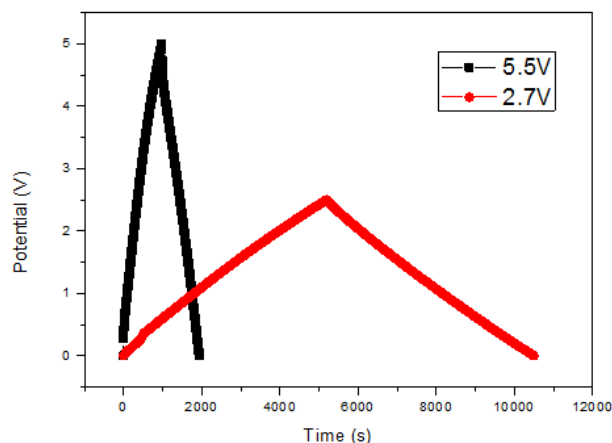
Table 1 lists the specific capacitance values that were calculated using the CV curves (equation (1)) and the mass of active material in each electrode. As expected, the specific capacitance decreased with increasing scan rate. The 10 F/2.7 V supercapacitor showed higher specific capacitance values that were significantly less dependent on the scan rate.

Figure 3 shows the charge/discharge curves for the 1 F/5.5 V and 10 F/2.7 V supercapacitors at room temperature. Both supercapacitors show almost linear charge and discharge behaviors.

**Table 1.** Specific capacitance values calculated using the areas of the CV curves.

| Rate<br>(Vs <sup>-1</sup> ) | Capacitor 1 F/5.5 V |                                    | Capacitor 10 F/2.7 V |                                    |
|-----------------------------|---------------------|------------------------------------|----------------------|------------------------------------|
|                             | CV integral         | C <sub>s</sub> (Fg <sup>-1</sup> ) | CV integral          | C <sub>s</sub> (Fg <sup>-1</sup> ) |
| 10                          | 0.0816              | 75.2                               | 0.4326               | 115.2                              |
| 20                          | 0.1235              | 55.2                               | 0.8933               | 119.2                              |
| 50                          | 0.1565              | 28.0                               | 2.0316               | 108.4                              |

Table 2 shows the specific capacitance values that were calculated using these curves (equation (2)) and the mass of active material in each electrode. Again, the 10 F/2.7 V supercapacitor showed a much higher specific capacitance (141.6 Fg<sup>-1</sup>); this value is higher than that achieved during the CV measurements at any scan rate. In contrast, the specific capacitance value of the 1 F/5.5 V supercapacitor (42.4 Fg<sup>-1</sup>) was lower than those achieved using CV at scan rates of 10 and 20 Vs<sup>-1</sup> (i.e., 72.2 and 55.2 Fg<sup>-1</sup>, respectively).



**Fig. 3.** Galvanostatic curves for the 1 F/5.5 V and 10 F/2.7 V supercapacitors.

**Table 2.** Specific capacitance values calculated using the galvanostatic cycles.

| Nominal capacitance (F) | $\Delta V$ (V) | $\Delta t$ (s) | Calculated $C_s$ ( $Fg^{-1}$ ) |
|-------------------------|----------------|----------------|--------------------------------|
| 1                       | 5.0            | 951.457        | 42.4                           |
| 10                      | 2.5            | 5312.01        | 141.6                          |

The parameters used for the calculations of the ESR values of the investigated supercapacitors are given in Tables 3 and 4. As expected, the performance of the 10 F/2.7 V supercapacitor was superior to that of the 1 F/5.5 V supercapacitor: The ESR values were 0.4 and 4.4  $\Omega$  per electrode for the 10 and 1 F supercapacitors, respectively. Since the ESR of the 1 F supercapacitor is almost 10 times that of the 10 F supercapacitor, this difference is significant and was quite visible in the CV curves.

**Table 3.** ESR values calculated for the 1 F supercapacitor.

| <b>ESR<sub>mean</sub> = ~4.4 <math>\Omega</math> per electrode</b> |       |       |       |
|--|-------|-------|-------|
| $V_f$ (V)  | 1.019 | 3.015 | 4.018 |
| $V_{min}$ (V)  | 0.999 | 3.000 | 4.000 |
| $i$ (A)  | 0.001 | 0.001 | 0.001 |
| ESR ( $\Omega$ )   | 20    | 15    | 18    |

**Table 4.** ESR values calculated for the 10 F supercapacitor.

| <b>ESR<sub>mean</sub> = 0.4 <math>\Omega</math> per electrode</b> |       |       |       |
|---|-------|-------|-------|
| $V_f$ (V)   | 1.010 | 2.005 | 3.008 |
| $V_{min}$ (V)   | 1.000 | 2.000 | 3.000 |
| $I$ (A)   | 0.010 | 0.010 | 0.010 |
| ESR ( $\Omega$ )  | 1.0   | 0.5   | 0.8   |

Figures 4 and 5 show the self-discharge curves of both supercapacitors at room temperature and close to the freezing point, respectively. The values for the parameters that were obtained from these curves and used to calculate the EPR values, are given in Tables 5 and 6. The EPR value of the 1 F/5.5 V supercapacitor (5.5 M $\Omega$  per electrode) was much higher than that of the 10 F/2.7 V supercapacitor (200 k $\Omega$  per electrode). The 1 F/5.5 V supercapacitor had an extremely high EPR value at temperatures close to the freezing point (59.5 M $\Omega$  per electrode).

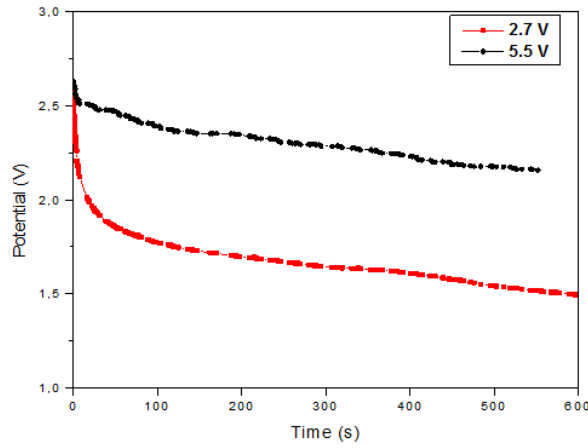


**Fig. 4.** Self-discharge curves of the carbon-based supercapacitors at room temperature.

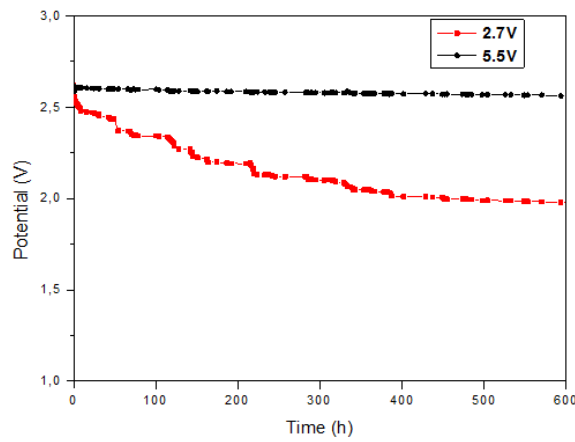


**Fig. 5.** Self-discharge curves of the carbon-based supercapacitors at 333 K.

**Table 5.** EPR values calculated for the supercapacitors at freezing point.

| Parameters                        | 10 F/2.7 V          | 1 F/5.5 V           |
|-----------------------------------|---------------------|---------------------|
| t (s)                             | $2.172 \times 10^6$ | $2.442 \times 10^6$ |
| C (F)                             | 10.0                | 1.0                 |
| $V_0$ (V)                         | 1.909               | 2.559               |
| V (V)                             | 2.622               | 2.612               |
| <b>EPR (M<math>\Omega</math>)</b> | <b>0.7</b>          | <b>119</b>          |

**Table 6.** EPR values calculated for the supercapacitors at room temperature.

| Parameters                        | 10 F/2.7 V          | 1 F/5.5 V           |
|-----------------------------------|---------------------|---------------------|
| t (s)                             | $2.183 \times 10^6$ | $2.193 \times 10^6$ |
| C (F)                             | 10.0                | 1.0                 |
| $V_0$ (V)                         | 1.491               | 2.158               |
| V (V)                             | 2.624               | 2.632               |
| <b>EPR (M<math>\Omega</math>)</b> | <b>0.4</b>          | <b>11.0</b>         |

Figure 6 shows micrographs of the composite material that comprised the electrodes of these supercapacitors. No significant morphological differences were evident in the scanning electron microscopy (SEM) results at these standard magnifications.

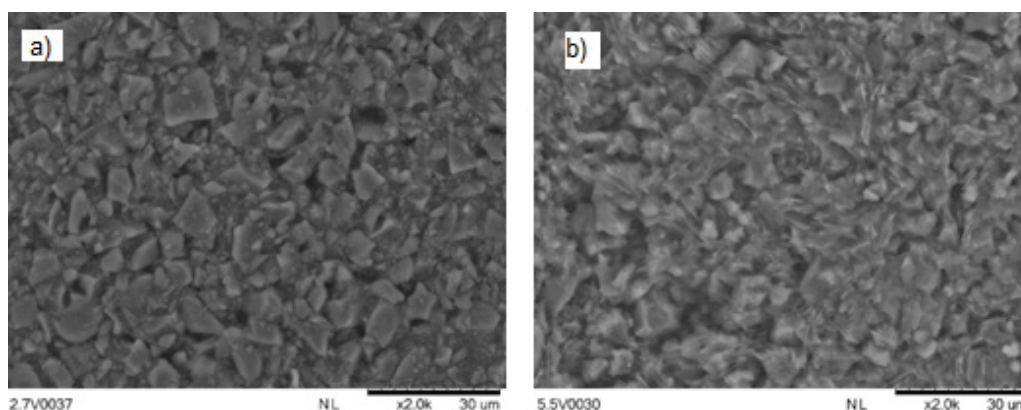


**Fig. 6.** SEM micrographs of the (a) 1 F and (b) 10 F supercapacitors.

## Conclusion

The results showed that the performances of commercial supercapacitors with different specific capacitances can differ considerably. The electrochemical characteristics of a tubular-type 10 F/2.7 V supercapacitor were superior to those of a disc-type 1 F/5.5 V supercapacitor. The 10 F supercapacitor featured a CV loop shape that was close to that of an ideal supercapacitor and a good ESR ( $0.4 \Omega$  per electrode); however, the 1 F supercapacitor had a higher EPR ( $11 \text{ M}\Omega$  per electrode). Temperature had a remarkable effect on the EPR of the disc-type 1 F/5.5 V supercapacitor. The specific capacitance of the electrode active material was significantly superior in the tubular-type 10 F/2.7 V supercapacitor.

## Acknowledgements

The authors would like to thank IPEN-CNEN/SP for supporting this investigation and the PIBIC-PROBIC program for a research grant (T. C. Gonsalves). In addition, the authors wish to thank the Federal Institute of Education, Science, and Technology of Rondônia Campus Porto Velho Calama for their financial support.

## References

- [1] M. Monte: Fuel Cells Vol. 10 (2010), p. 806.
- [2] C. Arbizzani, M. Mastragostino, F. Soavi: J. Power Sources Vol. 100 (2001), p. 164.
- [3] E. Frackowiak, F. Béguin: Carbon Vol. 39 (2001), p. 937.
- [4] A. Burke: J. Power Sources Vol. 91 (2000), p. 37.
- [5] D. Qu, H. Shi: J. Power Sources Vol. 74 (1998), p. 99.
- [6] J. Gamby, P. L. Taberna, P. Simon, J. F. Fauvarque, M. Chesneau: J. Power Sources Vol. 101 (2001), p. 109.
- [7] B. W. Ricketts, C. TonThat: J. Power Sources Vol. 89 (2000), p. 64.
- [8] Y. Wang: *Modeling of ultracapacitor short-term and long term dynamic behavior*. Master of Science Thesis, University of Akron (2008), p. 18.
- [9] G. Park: *Graphite: application to anode and cathode materials for energy storage device*. Doctoral Thesis, Saga University (2010), p. 19.
- [10] A. K. Shukla, A. Banerjee, M. K. Ravikumar, A. Jalajakshi: Electrochimica Acta Vol. 84 (2012), p. 165.